Heterogeneity and Dynamics of Lateral Line Afferent Innervation During Development in Zebrafish (*Danio rerio*)

Melanie Haehnel, Masashige Taguchi, and James C. Liao*

The Whitney Laboratory for Marine Bioscience, Department of Biology, University of Florida, St. Augustine, Florida 32080

ABSTRACT

The lateral line system of larval zebrafish is emerging as a model to study a range of topics in neurobiology, from hair cell regeneration to sensory processing. However, despite numerous studies detailing the patterning and development of lateral line neuromasts, little is known about the organization of their connections to afferent neurons and targets in the hindbrain. We found that as fish grow and neuromasts proliferate over the body surface, the number of afferent neurons increases linearly. The number of afferents innervating certain neuromasts increases over time, while it decreases for other neuromasts. The ratio of afferent neurons to neuromasts differs between the anterior and posterior lateral line system, suggesting potential differences in sensitivity threshold or spatial resolution. A single afferent neuron routinely contacts a group of neuromasts, suggesting that different afferent neurons can convey information about receptive fields along the body. When afferent projections are traced into the hindbrain, where a distinct somatotopy has been previously described, we find that this general organization is absent at the Mauthner cell. We speculate that directional input from the lateral line is less important at an early age, whereas the speed of the escape response is paramount, and that directional responses arise later in development. By quantifying morphological connections in the lateral line system, this study provides a detailed foundation to understand how hydrodynamic information is processed and ultimately translated into appropriate motor behaviors. J. Comp. Neurol. 520:1376–1386, 2012.

INDEXING TERMS: afferent neuron; Mauthner cell; neuromast; plasticity; somatotopy

The zebrafish lateral line system is emerging as a model to study fundamental questions in neurobiology, from sensory processing to neuronal path finding and somatotopy (Metcalfe et al., 1985; Alexandre and Ghysen, 1999; Liao, 2010; Sato et al., 2010). The lateral line system consists of sensory units called neuromasts, which are distributed along the body and head. Upon appropriate deflection by water flow, hair cells which are found in the neuromasts depolarize and release neurotransmitter onto afferent neuron terminals, which in turn convey this information to the hindbrain (Corey and Hudspeth, 1979; Howard and Hudspeth, 1987; Raible and Kruse, 2000; LeMasurier and Gillespie, 2005; Liao, 2010). Each neuromast contains two populations of hair cells with opposing polarities (Flock and Wersall, 1962). Afferent neurons connect specifically to hair cells of one polarity, both within and across neuromasts (Nagiel et al., 2008, 2009; Faucherre et al., 2009). The lateral line system on the trunk develops from well-defined migrating primordia, which differentiate into the individual neuromasts in a series of developmental waves (Harrison, 1904; Wright, 1951; Sapède et al., 2002; Nuñez et al., 2009; Sarrazin et al., 2010). In larval zebrafish these neuromasts are deposited in an organized sequence and can be individually identified (Raible and Kruse, 2000; Ghysen and Dambly-Chaudière, 2004; Nuñez et al., 2009; Sarrazin et al., 2010).

Zebrafish larvae possess all the components for a functional lateral line system at the time of hatching. The lateral line system must continue to detect water flow even as fish grow substantially in size and change in shape.

Grant sponsor: National Institutes of Health; Grant number: NIH RO1 DC 010809 (to J.C.L.).

*CORRESPONDENCE TO: James C. Liao, Whitney Laboratory for Marine Bioscience, University of Florida, 9505 Ocean Shore Blvd., St. Augustine, FL 32080. E-mail: jliao@whitney.ufl.edu

Received August 30, 2011; Revised October 4, 2011; Accepted October 25, 2011

DOI 10.1002/cne.22798

Published online November 18, 2011 in Wiley Online Library (wileyonlinelibrary.com)

While the patterning of neuromasts along the body has been described (Ledent, 2002; Nuñez et al., 2009), what is lacking is a quantification of neuromast numbers and their innervations by afferent neurons. The lateral line system can be subdivided into the anterior lateral line system, with afferent neurons innervating the cranial neuromasts (Raible and Kruse, 2000), and the posterior lateral system, with neurons innervating the neuromasts on the trunk via the lateral line nerve (Metcalfe et al., 1985). The afferent neurons project into the hindbrain where they establish a somatotopic organization (Alexandre and Ghysen, 1999). One direct postsynaptic target in the hindbrain is the Mauthner cell, which is a paired structure responsible for mediating the escape response in fishes (Korn et al., 1974; Faber and Korn, 1975). It remains unknown how afferent neurons innervating neuromasts in different locations on the trunk connect to the Mauthner cell and if a somatotopic organization is evident along its lateral dendrite. It is generally assumed that these innervations are established early in development since fast escape responses are crucial for the survival of the larval fishes (Nissanov et al., 1999). The aim of this study is to present data that will lay the groundwork for understanding how hydrodynamic stimuli may be encoded and to provide a basis to interpret future physiological studies (Metcalfe et al., 1985; Alexandre and Ghysen, 1999; Liao, 2010; Sato et al., 2010).

MATERIALS AND METHODS

Zebrafish strains and husbandry

Zebrafish were bred from laboratory stocks and maintained at 28.5°C on a 14/10-hour light/dark cycle. All protocols were approved by the University of Florida and according to our Institutional Animal Care and Use Committee (IACUC) and National Institutes of Health (NIH) guidelines. Eggs and larvae were maintained in 10% Hank's solution (137 mM NaCl, 5.4 mM KCl, 1 mM $MgSO_4$, 0.44 mM KH_2PO_4, 0.25 mM Na_2HPO_4, 4.2 mM $NaHCO_3$, 1.3 mM $CaCl_2$) in an incubator (Tritech Research, Los Angeles, CA) at 28.5°C and a density of 50–100 per 100-mm Petri dish (Falcon, Optilux Petri Dish, Becton Dickinson, Franklin Lakes, NJ). Larvae older than 5 days were transferred to nursery tanks in the system (Aquatic Habitats, Apopka, FL).

The transgenic strain HuC:Kaede, which expresses the photo-convertible protein Kaede throughout the nervous system (Sato et al., 2006), was obtained from the Laboratory for Developmental Gene Regulation (Riken Brain Science Institute, Japan). The nacre mutant line, which lacks melanin, was obtained from the Fetcho Laboratory (Cornell University, Ithaca, NY). Wildtype fish were obtained from a local pet store.

Neuromast imaging

Neuromasts were labeled with the fluorescent dye 2-[4-(dimethylamino)styryl]-1-ethylpyridinium iodide (DASPEI; Molecular Probes, Eugene, OR). Embryos were first anesthetized in 0.16% tricaine methanesulfonate (MS-222, Finquel, Argent, Redmond, WA) and then immersed in 0.5 mM DASPEI. After 10 minutes fish were rinsed three times and mounted in 1.4% low melting point agar (Fisher Scientific, Fair Lawn, NJ). All solutions were prepared with Hank's solution at pH 7. Neuromasts were imaged under an Olympus MV X10 epifluorescence microscope (Tokyo, Japan) equipped with an Olympus U-MRFPHQ/XL RFP filter to visualize DASPEI fluorescence at 63× magnification. Images of the neuromast distribution across fish ages were acquired using an Olympus DP 70 digital camera. The size of the fish was measured with a ruler under the microscope.

Lateral line afferent neurons

To reliably identify and count the somata of lateral line afferent neurons in the anterior (ALL) and posterior lateral line (PLL) ganglion we used HuC:Kaede larvae, which express fluorescent protein in ALL neurons. First, larvae at different stages of development were anesthetized and mounted in agar with their side against the bottom of a microscope slide dish (FluoroDish, World Precision Instruments, Sarasota, FL). Next, fluorescence was imaged under a Leica SP5 confocal microscope (Leica Microsystems, Wetzlar, Germany) with a Leica HCX PL APO X63/1.20 NA water immersion objective and settings for FITC/TRITC visualization (541/572 nm excitation/emission and 494/518 nm excitation/emission, respectively). Optical sections (2 μm) were taken at 1024 × 1024 pixel resolution. Image stacks were then imported into ImageJ where somata were marked and counted (ROI manager tool, NIH, http://rsb.info.nih.gov/ij/). In order to eliminate potential bias, this procedure was carried out single-blind such that the observer did not know the age of the fish.

Electroporation

In order to label afferent neurons that innervate different neuromasts, as well as to label the Mauthner cell, somata were backfilled with fluorescent dyes using an Axoporator 800A (Molecular Devices, Sunnyvale, CA). Pipettes for electroporation were pulled from borosilicate glass (G150F-3, inner diameter: 0.86 mm, outer diameter: 1.50 mm, Warner Instruments, Hamden, CT) with a P97 puller (Sutter Instruments, Novato, CA) to resistances of 3–10 MΩ. Pipettes were mounted to a head stage (AP-1A-1MU, Molecular Devices) and positioned using a four axis electric micro stepper (Siskiyou, Grants Pass, OR).

Larvae were anesthetized and mounted near the surface of the agar in a slide dish. Neuromasts were located with Nomarski optics under an Olympus BX51WI fluorescent microscope with an ×40/0.80 NA Olympus Plan F1 water immersion objective. Images were taken with a CCD camera mounted onto the microscope (Rolera XR Fast1349, QImaging, Surrey, BC, Canada).

Afferent neurons were electroporated with tetramethyl rhodamine dextran or Alexa 647 dextran (10,000 MW; Molecular Probes) by bringing the pipette to the surface of a neuromast and applying the following positive/negative square pulse protocol: voltage = 50–100 mV, train duration = 5 sec, frequency = 20 Hz, pulse width 5.5 ms. The Mauthner cell was electroporated with Alexa 488 dextran (10,000 MW; Molecular Probes) by bringing the pipette close to the Mauthner cell axon in the spinal cord and applying the same pulse protocol described above. Somata of electroporated afferents were observed and counted using a Texas Red filter (Olympus 41004 TR C127531) and Cy5 filter (Olympus 41024 C5 LP C127409) while the Mauthner cell was observed using a GFP filter (Olympus 41018 EGFP C127532). After electroporation, fish were removed from the agar and kept in Hank's solution for image acquisition with a confocal microscope at a later timepoint.

Visualization and analysis of post-synaptic lateral line targets

We used a Leica SP5 confocal microscope to image the putative postsynaptic targets of afferent hindbrain projections by positioning fish in agar with their dorsal side down against a microscope slide dish. Optical stacks were acquired with 1-μm steps, 1024 × 1024 pixel resolution and settings for TRITC/FITC/Cy5 (650/670 nm excitation/emission). Images were imported into ImageJ for further analysis. To determine the spatial distribution of afferent central projections relative to the Mauthner cell, the channels for the three wavelength spectra were analyzed separately. Afferents innervating the D2 and L1 or L5 neuromast were labeled with rhodamine and Alexa 647 dextran, respectively, while the Mauthner cell was labeled with Alexa 488. All structures not contiguous with the Mauthner cell or the afferent neurons were excluded from the analysis. The contrast of the entire image stack was autoadjusted and each section was filtered with a 3-pixel radius median filter. The stack was then converted to a binary image and the pixel area of the stained structure was expressed as percentage of the total pixel number for each section. For each section the area covered by the stained structure was normalized to the section that contained the maximum area covered by the structure. This was done so that sections containing both large and small stained areas could be compared for the entire image stack. The dorsoventral position of the afferent projections in relation to the Mauthner cell was determined by comparing the distance between the sections containing the largest area covered by each structure. Where appropriate, stacks were rotated using Leica Confocal Software.

Statistical analysis and figure production

All graphs, statistical tests, and calculations were performed in MatLab R2009b (MathWorks, Natick, MA). Lines of best fit were calculated based on a linear model and the significance of correlations was determined with a *t*-statistic. A one-way analysis of variance (ANOVA) with a Bonferroni post-hoc test was used to determine differences in the number of afferents innervating different neuromasts. A Wilcoxon signed-rank test was used to compare the relative dorsoventral distance between afferent projections and the Mauthner cell. For all tests significance was reported at $P < 0.05$. Figure schematics were produced by digitizing the outlines of fish images taken with an Olympus DP 70 digital camera in CorelDraw X5 (Corel, Ottawa, Canada). When necessary, brightness and contrast were systematically adjusted in ImageJ for the entire image. Final figures were assembled using Adobe Illustrator CS5 V 15.0.0 (Adobe Systems, San Jose, CA).

RESULTS

Organization of the lateral line system and neuromast distribution

We identified neuromasts in the ALL and PLL following terminology used in earlier studies (Metcalfe et al., 1985; Raible and Kruse, 2000; Ledent, 2002; Nuñez et al., 2009; Sarrazin et al., 2010). The PLL system comprises dorsal (D-) and lateral (L-) neuromasts on the trunk, derived from the PLL primordia, which also give rise to PLL afferent neurons located in the PLL ganglion posterior to the otic capsule (Sapède et al., 2002). The ALL system consists of neuromasts on the head which lie along the supraorbital, infraorbital, mandibular, opercular, and otic branches of the ALL nerve. This nerve contains the afferent projections of the ALL originating from the ALL ganglion located anterior to the otic capsule (Raible and Kruse, 2000). Figure 1 shows the overall organization of the lateral line neuromasts in 3–40 days postfertilization (dpf) old fish. At 55 hours postfertilization (hpf) larvae have hatched from the chorion and the first neuromasts have differentiated and are visible (Fig. 1A). The PLL consisted typically of three neuromasts (L1-L3) located along the midline of the body. Two ALL neuromasts become visible on the head. At 3 dpf we counted eight lateral

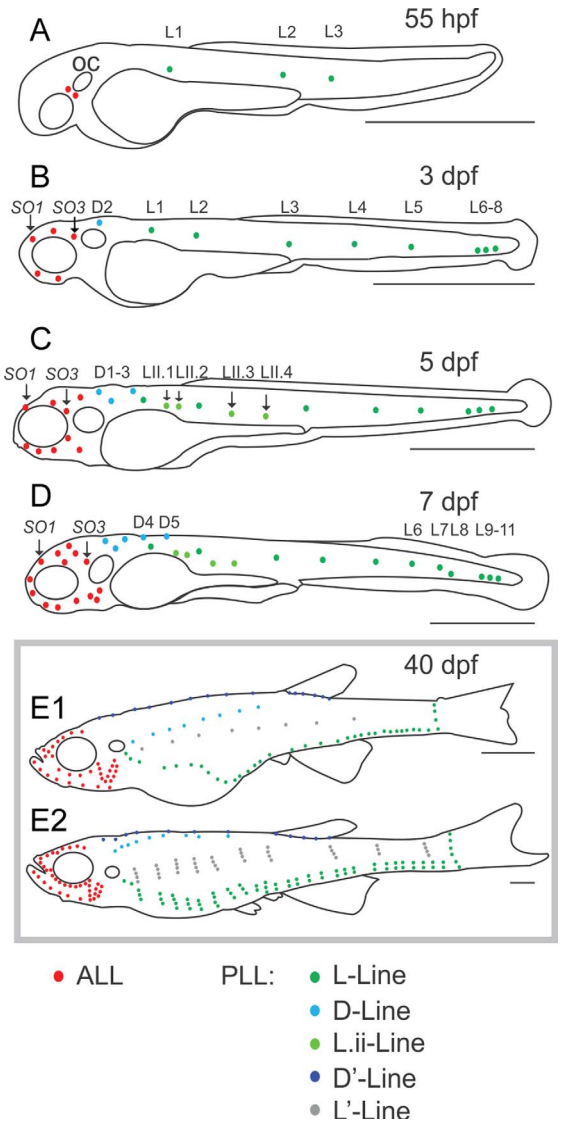

Figure 1. Pattern of neuromast distribution in larval and juvenile zebrafish. **A:** At 55 hours postfertilization (hpf) the first neuromasts of the posterior lateral line (PLL, L1-3: green) and the anterior lateral line (ALL, red) appear. **B:** At 3 days postfertilization (dpf) there are eight neuromasts along the midline (L1-8). Note that the first dorsal neuromast to appear in the PLL is D2 (blue). The number of neuromasts in the ALL has increased (supraorbital neuromasts 1 and 3 are marked: SO1, SO3). **C:** At 5 dpf neuromasts derived from a second PLL-primordium develop (LII.1-4: light green) and are inserted between L1 and L2, as well as L3 and L4. There are three neuromasts in the dorsal branch of the PLL (D1 and D3). The number of ALL neuromasts has increased below the eye. **D:** At 7 dpf there are ≈15 lateral neuromasts in the PLL and five dorsal neuromasts. There are 14 neuromasts in the ALL. **E:** Simplified schematic of neuromast distribution in postlarval fish of the same age (40 dpf) but different size with different numbers of neuromasts. For example, an 8-mm long fish (E1) possesses much fewer neuromasts than a 16-mm long fish (E2). New lateral neuromasts have formed (L' neuromasts: gray) above the original L-line. Neuromasts in the longer fish have proliferated to form dorsoventral stitches from the L' and L neuromasts (Nuñez et al., 2009). New dorsal neuromasts have begun to form above the original D-line in both fish (D' neuromasts: dark blue). Scale bars = 1 mm.

neuromasts in the PLL (L1-L8; Fig. 1B). Neuromasts L1-L5 were distributed along the midline, while neuromasts L6-L8 were found more ventrally (Sapède et al., 2002). The first dorsal neuromast (D2) of the PLL had also appeared at this time. The number of neuromasts in the ALL had increased, following the supraorbital and the infraorbital branches of the ALL nerve. Along the supraorbital branch the rostralmost neuromast was labeled SO1 and the neuromast located closest to the ALL ganglion was referred to as SO3. These neuromasts of the ALL could be reliably identified across individuals and were targeted in later experiments. At 5 dpf, LII-neuromasts derived from a second PLL-primordium (Sapède et al., 2002; Sarrazin et al., 2010) were inserted between L1 and L2, as well as between L3 and L4 (Fig. 1C). We counted three dorsal neuromasts in the PLL (D1-D3). In the ALL, the number of neuromasts had increased to 10. At 7 dpf, there were typically about 15 lateral neuromasts in the PLL (Fig. 1D) and new dorsal neuromasts were added. The number of neuromasts in the ALL had increased to 14.

Fish of the same age begin to differ in size after the onset of exogenous feeding (Schilling, 2002) For example, 8-mm-long fish (Fig. 1E1) had fewer neuromasts than 16-mm-long fish of the same age (Fig. 1E2). In 16-mm fish the lateral neuromasts in the PLL (L-line) had proliferated to form small linear series, called stitches (Ledent, 2002; Nuñez et al., 2009). New lateral neuromasts, also organized into stitches, formed ventral to the initial L-line along with a new dorsal line above the initial D-line. In comparison, in 8-mm fish the new L-line had formed, but neuromasts had not yet proliferated into stitches.

Neuromast proliferation during development

To determine the developmental dynamics of the lateral line system, we first counted ALL and PLL neuromasts in 2–7 dpf wildtype larvae. Immediately after hatching at 2 dpf, the PLL and ALL each contained up to three neuromasts. During the first 7 dpf, neuromasts were added to the ALL and PLL at a rate of about three neuromasts per day (Fig. 2A). Up to an age of 7 dpf, both age and size were good predictors for neuromast number because larvae of the same age did not differ substantially in size (Fig. 2B). In the following sections we will use age to characterize the developmental progress of the lateral line system in fish up to 14 dpf, since age was more reliable to measure. We found that size was correlated with neuromast number for fish growing past this stage and that more neuromasts were added to the PLL than to the ALL (Fig. 2C,D).

Development of afferent innervations

The ganglion containing the cell bodies of the ALL afferent neurons is located rostral to the otic capsule, caudal

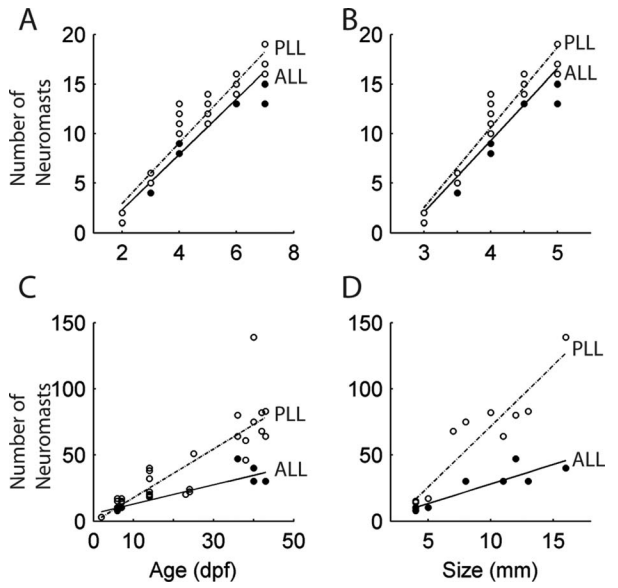

Figure 2. The number of neuromasts on the body increases in larvae and juveniles with age. **A:** In 2–7 dpf larvae the number of neuromasts increases linearly in the ALL (black circles, solid line) and the PLL (white circles, dashed line). Approximately three new neuromasts are added each day to the ALL and PLL; $y_{ALL} = 2.8x - 3.3$, $R^2_{ALL} = 0.95$, $p_{ALL} < 0.0001$, $y_{PLL} = 3.1x - 3.2$, $R^2_{PLL} = 0.93$, $p_{PLL} < 0.0001$ ($n = 30$). **B:** Neuromast number also increases as a function of body size. For each 1 mm increase in body size around seven neuromasts are added to the ALL and eight to the PLL; $y_{ALL} = 7.2x - 19.7$, $R^2_{ALL} = 0.91$, $p_{ALL} < 0.0001$, $y_{PLL} = 8.1x - 21.72$, $R^2_{PLL} = 0.92$, $p_{PLL} < 0.0001$ ($n = 30$). Thus, for early stage larvae there is not much difference in age and size, so either can be used to predict neuromast number. In contrast, an analysis including older fish shows that age and size are not as well correlated. **C:** Neuromast proliferation until 43 dpf. The proliferation of neuromasts differs substantially between the ALL and PLL after the first few days of development because in older fish body size can differ greatly; $y_{ALL} = 0.7x + 5.5$, $y_{PLL} = 1.8x - 0.9$, $R^2_{ALL} = 0.8$, $p_{ALL} < 0.001$, $R^2_{PLL} = 0.7$, $p_{PLL} < 0.0001$ ($n = 22$). **D:** Across a wider range of developmental stages, it becomes clear that body size is a better predictor than age for the number of PLL neuromasts on the body; $y_{ALL} = 3.0x - 1.8$, $R^2_{ALL} = 0.8$, $p_{ALL} < 0.001$, $y_{PLL} = 9.2x - 20.3$, $R^2_{PLL} = 0.9$, $p_{PLL} < 0.0001$ ($n = 9$).

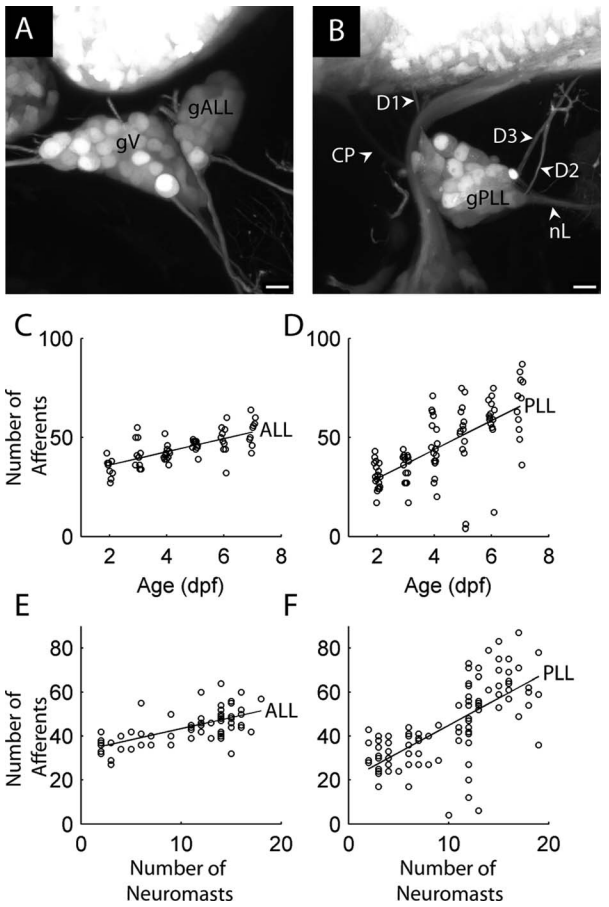

Figure 3. The number of afferent neurons relative to neuromasts increases during development. **A:** Confocal stack (≈60 μm) showing afferent neurons in the ALL ganglion (gALL) at 3 dpf; gV: trigeminal ganglion. Anterior is to the left and dorsal to the top. **B:** Confocal stack (≈60 μm) showing afferent neurons of the PLL ganglion (gPLL) at 3 dpf. Arrows indicate PLL-projections to dorsal neuromasts (D1, D2, and D3). nL, lateral branch of the PLL nerve that projects down the body; CP, central projections to hindbrain. **C:** The number of afferent neurons in the ALL ganglion plotted against fish age: $y = 3.3x + 29.4$, $R^2 = 0.5$, $P < 0.0001$ ($n = 65$). **D:** Number of afferents in the PLL ganglion plotted against age: $y = 7.34x + 14.4$, $R^2 = 0.5$, $P < 0.0001$ ($n = 94$). **E:** Number of afferent neurons plotted against the number of neuromasts for 2-7 dpf fish: $y = 1.0x + 33.3$, $R^2 = 0.4$, $P < 0.0001$. **F:** Number of afferent neurons in the PLL ganglion plotted against the number of neuromasts for 2–7 dpf fish: $y = 2.5x + 20.2$, $R^2 = 0.5$, $P < 0.0001$. Scale bars = 10 μm.

to the eye and dorsal of the trigeminal ganglion (Fig. 3A). The PLL ganglion is located caudal to the otic capsule and rostral to the cleithrum (Fig. 3B). Isolated PLL afferent projections innervate the dorsal neuromasts (white arrowheads in Fig. 3B), while the axons innervating the lateral neuromasts run together in the lateral line nerve. The number of afferent neurons in the ALL and the PLL increased linearly with age (Fig. 3C,D). There was more variation in the number of afferent neurons in the PLL than in the ALL for a given age (Fig. 3E,F). We estimated that about 33 neurons were initially present in the ALL ganglion. For each neuromast added to the ALL, one afferent neuron was added (Fig. 3E). In the PLL fewer afferent neurons (≈20) were initially present in the ganglion (Fig. 3F). For each neuromast that was added to the PLL, 2–3 afferent neurons were added.

Afferent innervations in different neuromasts lines on the head and trunk

To address the question of whether neuromasts in different locations of the body were innervated by different numbers of afferent neurons during development, we

electroporated fluorescent dye into selected neuromasts (Fig. 4A,B1). After electroporation the labeled cell bodies could be identified in the ganglion and counted (Fig. 4B2). The number of afferent neurons contacting the SO1 neuromast in the ALL decreased with age (Fig. 4C), while the number of afferents contacting the SO3 did not (Fig. 4D). For the dorsal neuromasts of the PLL, the number of afferents contacting the D1 neuromast did not change with age (Fig. 4E), while the number of afferents contacting the D2 neuromast decreased (Fig. 4F). The number of afferents contacting the L1 neuromast increased with age (Fig. 4G), while the number of afferents contacting the L5 neuromast did not change (Fig. 4H). When data were pooled for fish across all ages, we found that fewer afferents contacted the D1 neuromast than the SO1, SO2, and D2 neuromasts (Fig. 4I).

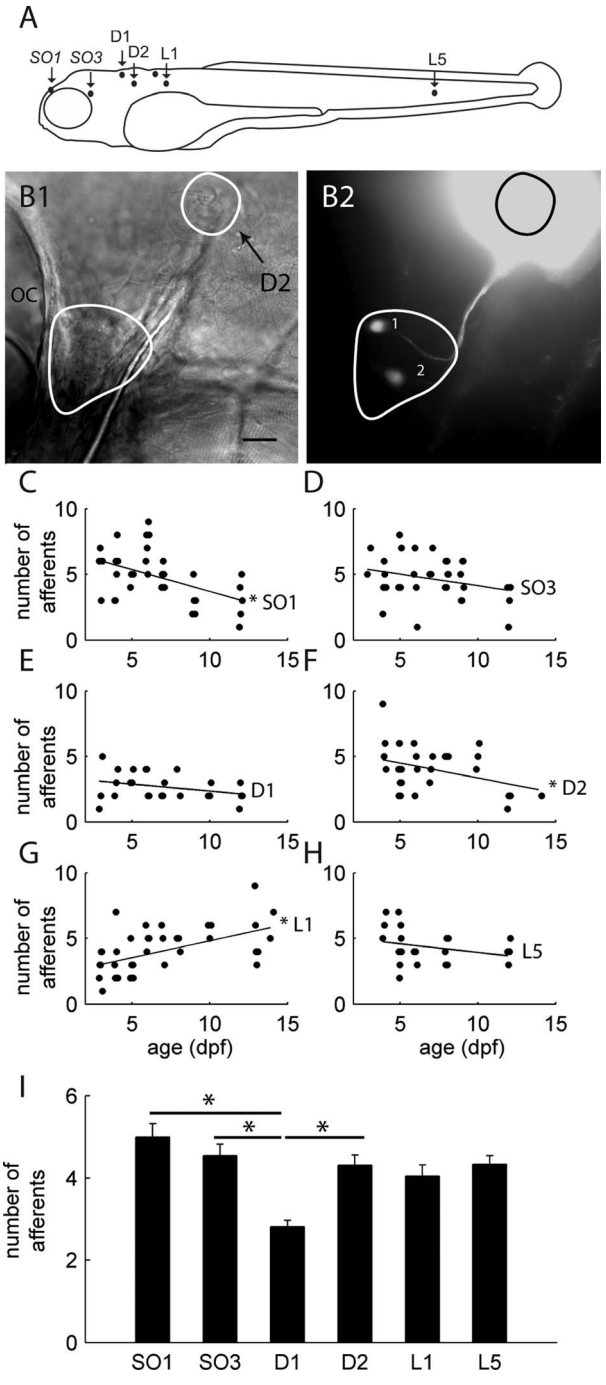

Postsynaptic targets of the lateral line afferents

We traced the central projections of afferent neurons into the hindbrain to look for somatotopic organization onto an identified postsynaptic target, the Mauthner cell, which mediates the escape response in fishes (Korn et al., 1974; Faber and Korn, 1975). We examined the relationship between the Mauthner cell and afferent neurons innervating L1, L5, and D2 neuromasts (Fig. 5A–C), and found that afferent projections come into close proximity with the distal end of the lateral dendrite of the Mauthner cell (Fig. 5D,E). When fish are viewed from the lateral side, it is clear that afferent neurons ascending from neuromasts D2 and L1 converge upon the contact area with the Mauthner cell. The robust somatotopic organization, whereby caudal neuromasts project more dorsally into the hindbrain than more rostral neuromasts (Alexandre and Ghysen, 1999), is less evident (Fig. 5F,G).

Figure 4. Variation in the number of afferent neurons that innervate selected neuromasts in the ALL and PLL. The number of neurons that contact a neuromast differs depending on the location of the neuromast on the body as well as the age of the fish. **A:** Schematic of those neuromasts backfilled to reveal afferent neurons that innervate them; L1, L5, D1, and D2 in the PLL system and SO1 and SO3 in the ALL system. **B1:** Differential interference contrast image showing the location of the D2 neuromast and the PLL ganglion (gPLL); OC, otic capsule. **B2:** Same image of B1 in fluorescence showing two afferent neurons innervating the D2 neuromast. **C:** The number of afferent neurons innervating the SO1 neuromast decreases significantly as fish develop from 3 to 12 dpf ($y = -0.3x + 7.0$, $R^2 = 0.24$, $P < 0.01$, $n = 36$). **D:** The number of afferents innervating the SO3 neuromast do not change significantly ($n = 37$). **E:** The number of afferent neurons innervating the D1 neuromast does not significantly change between 3 and 12 dpf, $n = 25$. **F:** The number of afferent neurons innervating the D2 neuromast decreases significantly between 4 and 12 dpf, $y = -0.2x + 5.6$, $R^2 = 0.13$, $P < 0.05$, $n = 32$. **G:** The number of afferents innervating the L1 neuromast increases significantly between 3 and 14 dpf, $y = 0.3x + 2.3$, $R^2 = 0.3$, $P < 0.001$, $n = 41$. **H:** The number of afferents innervating the L5 neuromast does not change significantly between 4 and 12 dpf, $n = 23$. **I:** Bar graph shows mean number (±SEM) of afferent neurons across all ages (3–14 dpf) innervating each neuromast. There are significant differences between the D1 and the SO1, SO3, and the D2 as indicated by asterisks (one way-ANOVA, $F = 4.47$, df = 5, $P < 0.001$, Bonferroni post-hoc test). Note that the different age ranges selected for each neuromast reflect the earliest or latest point during development at which the neuromast can be reliably identified. Scale bar = 20 μm.

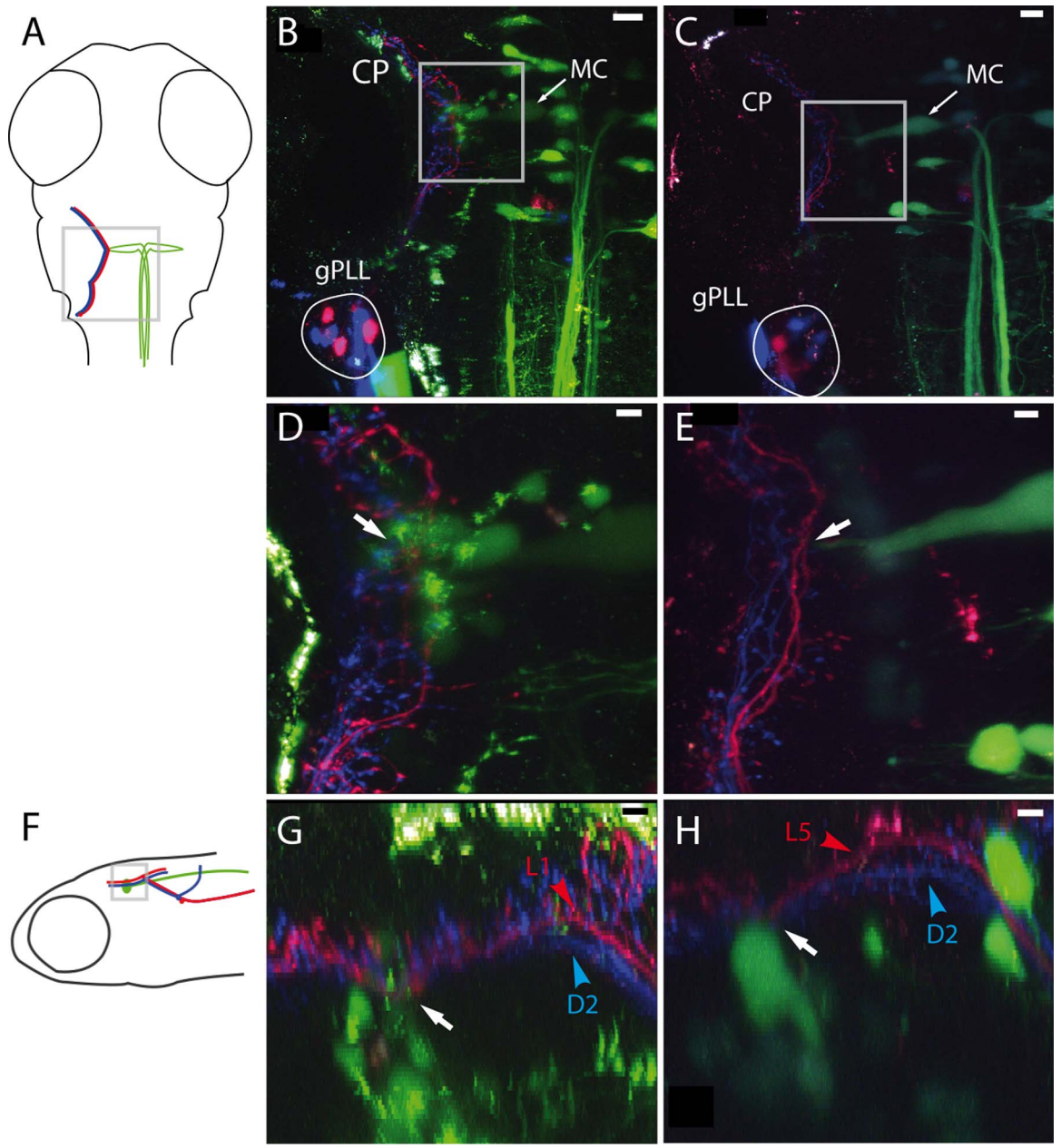

Figure 5. Lateral line afferent neurons send central projections into the hindbrain to contact the Mauthner cell in 5 dpf larvae. **A:** Dorsal schematic of the head corresponding to confocal stacks shown in B–E. The paired Mauthner cells are colored in green, the central projections of afferents innervating L1 or L5 in red, and the central projections of afferents innervating D2 in blue, as in the actual confocal images. The gray square outlines the area corresponding to panels B,C. **B:** The Mauthner cell (MC) and central projections of afferents (CP) innervating L1 and D2 are shown along with the PLL ganglion (gPLL). Square indicates region of detail in panel D. **C:** Central projections for L5 and D2. Square indicates region of detail in panel E. **D:** Afferent projections belonging to the L1 and D2 neuromast form putative contacts (arrow), with the lateral dendrite of the Mauthner cell. **E:** Afferent projections of the L5 and D2 intermingle less but also form putative contacts (arrow) with the lateral dendrite of the Mauthner cell. **F:** Lateral schematic of the head, where the gray square corresponds to panels G,H. **G:** Rotated view of the confocal stack in D, showing that afferent projections approach the lateral dendrite of the Mauthner cell (arrow). **H:** Rotated view of the confocal stack in E. Note that the central projections from L5 and D2 show a larger dorsoventral separation posterior to the point of contact (arrow) with the Mauthner cell. Scale bars = 20 μm in B; 5 μm in C-E,G,H.

This result is seen even for afferent neurons that ascend from more spatially separated neuromasts like D2 and L5 (Fig. 5H).

We analyzed the spatial relationship of the central projections relative to the Mauthner cell and found that the largest fraction of L1 and D2 projections were located

dorsal to the Mauthner cell (Fig. 6A). L1 and D2 projections partially overlapped throughout the distribution of their axon terminals and in the location where they contacted the Mauthner cell. The L5 neuromast is located more caudally along the body than the D2. The L5 projection into the hindbrain was found more dorsally with respect to the D2 projection (Fig. 6B). To quantify the spatial relationship between the afferent projections and the Mauthner cell we measured the peaks of the pixel distribution for the L1 and D2 and for the L5 and D2 projections with respect to the Mauthner cell but found no significant difference (Fig. 6C,D, respectively).

DISCUSSION

By quantifying the increase in the number of lateral line afferent neurons and neuromasts with age, we provide a detailed characterization of the development of neuromast innervations in a vertebrate hair cell system. We found that the stereotypical pattern of neuromast deposition found in previous studies on wildtype fish is also conserved in nacre and HuC:Kaede fish (Fig. 1). In larvae up to an age of 7 dpf, equal numbers of neuromasts are added to the anterior and posterior lateral line system (Fig. 2A,B). As the animal ages and grows, more neuromasts are added to the posterior lateral line system than to the anterior lateral line system, which may be correlated with the greater increase in body area compared to the head (Fig. 2C,D). This is consistent with earlier estimations that state that neuromasts increase with the square of the body size to represent flow in proportion to body surface area (Ghysen and Dambly-Chaudière, 2007).

Afferent innervation

When zebrafish hatch at 2 dpf, there are many more afferent neurons than neuromasts present in the anterior and posterior lateral line system. It is unclear if all these afferent neurons innervate neuromasts, given that primordia are still depositing new neuromasts (Sapède et al., 2002; Nuñez et al., 2009; Sarrazin et al., 2010). At 2 dpf the ratio between afferent neurons and neuromasts is higher in the anterior lateral line than in the posterior lateral line (Fig. 3C,D). During subsequent days' development more neuromasts are added to the posterior lateral line system (three afferent neurons for each new neuromast) than to the anterior lateral line (one afferent neuron for each new neuromast). As a consequence, the ratio between afferent neurons and neuromasts (approximately 3:1) is almost equal in the anterior and posterior lateral line at the oldest age investigated here (Fig. 3E,F). This ratio suggests a redundant innervation, whereby at least a group of neuromasts must be innervated by more

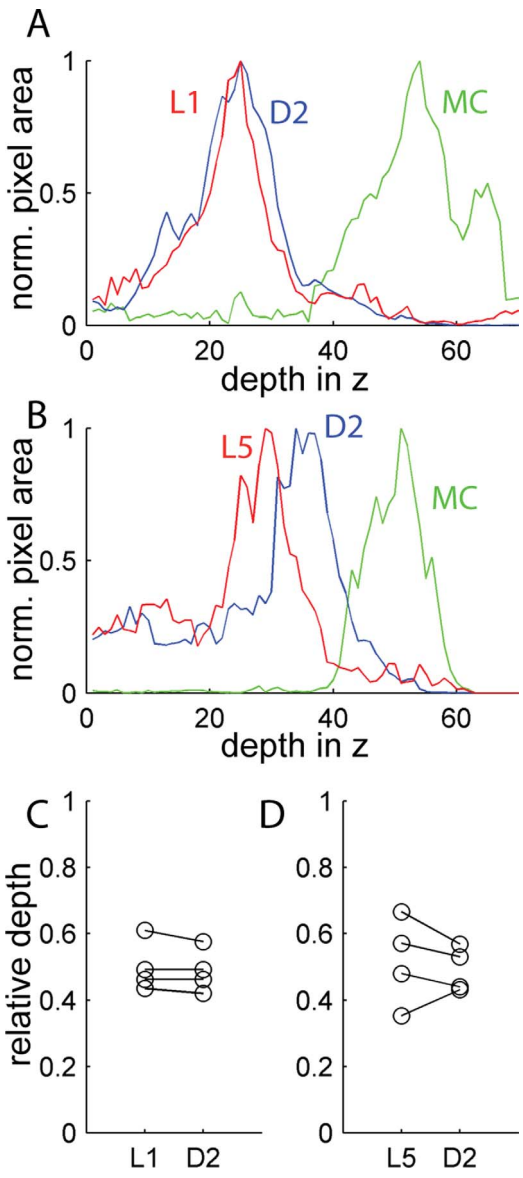

Figure 6. Dorsoventral position of afferent central projections showing distributions and regions of overlap with the Mauthner cell in the hindbrain of 5 dpf larvae. **A:** Profile of normalized pixel area indicating the depth of afferent projections belonging to the D2 (blue) and L1 (red) neuromasts relative to the Mauthner cell (green). The largest areas of projection for afferents contacting the L1 and D2 neuromast occupy a similar depth region, as indicated by the overlap in peak pixel area. The predominant locations of these central projections lie more dorsally than the main body of the Mauthner cell. **B:** Profile of normalized pixel area indicating the depth of afferent projections belonging to the D2 and L5 neuromasts relative to the Mauthner cell. The largest area of projection for the D2 afferent lies more ventral than the L5 afferent, and is located closer to, and overlaps more substantially with, the Mauthner cell. **C:** There is no significant difference between the largest areas of projection for the L1 and D2 afferents and the Mauthner cell ($n = 4$, Wilcoxon signed rank test). **D:** For three of the four cells tested, the largest area of projection for the D2 is substantially closer to the Mauthner cell than for the L5. One of the projections shows the reverse trend, where the projection for the D2 is farther from the Mauthner cell than the L5.

than two afferent neurons. If we assume neurons and neuromasts continue to be added to the anterior lateral line at the same rate, the ratio between afferents and neuromasts would eventually approach 1:1.

Figure 7 shows the different ratios of afferent neurons to the neuromasts they innervate that we observed in the lateral line system. Given that each neuromast contains two populations of hair cells of opposing polarizations, a neuromast must be innervated by at least two polarization-specific afferent neurons (Nagiel et al., 2008, 2009; Faucherre et al., 2009). Thus, if in the anterior lateral line system the ratio of afferent neurons to neuromasts approaches 1:1, each afferent should contact at least two neuromasts (Fig. 7A). We found that neuromasts in the anterior lateral line system are on average innervated by 4–6 afferent neurons, such that even more afferent neurons have to be shared between neuromasts (Fig. 4C,D,I). The greater potential for innervation redundancy in the posterior lateral line system implies that most neuromasts are innervated by more than two afferent neurons (compare also Fig. 4I). Therefore, it is likely that overlapping sets of afferent neurons sample information from several neuromasts (Fig. 7C). We propose that a group of neuromasts that are all innervated by a single afferent neuron can be considered the receptive field of that neuron. This suggests that an afferent receiving information from a group of neuromasts covering a certain body area can be treated as a functional unit with respect to their postsynaptic targets in the hindbrain.

We found that some neuromasts are exclusively innervated by their "own" afferent neurons, without evidence for sharing innervation with adjacent neuromasts (Fig. 7B). This was the case for the D1 neuromast in the posterior lateral line system, which is innervated by an average of two afferent neurons (Fig. 4I). It is likely for D1 that, given that it is the only neuromast with anterior–posterior polarization within an array of dorsoventrally polarized neuromasts (Sapède et al., 2002), it plays a unique role in the integration of flow information.

The fact that we find different patterns of innervations among neuromasts in different lines on the head and trunk raises the possibility of the existence of different neuromast types. For example, the different innervation patterns may reflect an early delineation into superficial and canal neuromasts (Webb and Shirey, 2003). Evidence for different types of neuromasts exists also in *Xenopus*, where afferent neurons that contact neuromasts in adjacent stitches are more sensitive than neurons that innervate only one stitch (Mohr and Görner, 1996). Perhaps, similar to *Xenopus*, certain neuromasts are more sensitive than others, although there are no data on zebrafish to support this at the moment. Another direction for future research could address whether this heterogeneity in

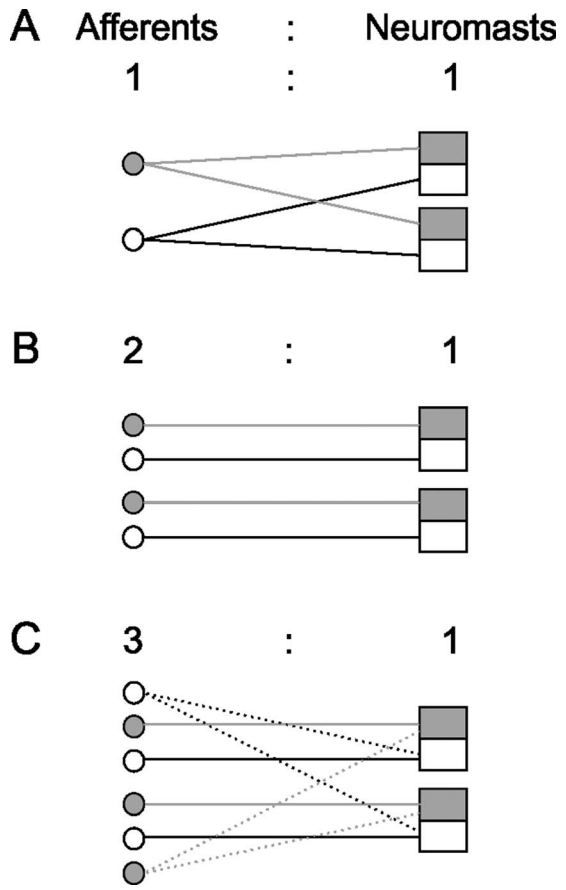

Figure 7. Schematic of possible afferent neuron to neuromast innervation patterns. Each neuromast contains hair cells with two polarizations, indicated in black and white. Hair cells of one polarization are innervated by a distinct population of afferent neurons, while hair cells of the opposite polarization are innervated by a separate population of neurons (Nagiel et al., 2008). **A:** Since afferent neurons innervating neuromasts with a 1:1 ratio and there are equal numbers of afferents and neuromasts, then each neuromast must be innervated by at least two afferent neurons and every afferent must be innervating at least two neuromasts. **B:** Afferent neurons and neuromasts occur with a 2:1 ratio. In every neuromast, hair cells of one polarization are innervated by a "designated" afferent neuron. Innervations do not necessarily overlap. This innervation pattern was pattern was found for the D1 neuromast, which is innervated by two afferent neurons, which are not shared by other neuromasts. **C:** Afferent neurons and neuromasts occur with a 3:1 ratio or higher. In this case, a group of neuromasts must be innervated by more than two afferent neurons. Dotted lines indicate possible innervations by additional afferent neurons; however, other innervation combinations are possible. This innervation pattern, which has the potential for the most redundancy, was found early in development when many more afferent neurons than neuromasts are present. It also may represent the situation in the posterior lateral line system later in development, where three afferents are added for each neuromast and a given neuromast is, on average, innervated by 4–6 neurons.

patterning is attributed to different polarization sensitivities later in development.

Developmental plasticity

We found that for some neuromasts the number of innervating afferent neurons increases over time, while for other neuromasts this number decreases or stays the same (Fig. 4C–H). Such plasticity in organization may result in changes in sensitivity and resolution as this modality matures and new components are added. For example, plasticity in the wind-sensitive cricket cercal system can occur when connections onto few early receptors, which are sufficient for the animal in the beginning of development, are followed by more complex innervation as the system becomes more advanced (Chiba et al., 1988). We can envision a similar mechanism in lateral line system development whereby early afferent innervation onto initial neuromasts are followed by more elaborate innervation patterns as more neuromasts are added to the system.

In other sensory systems plasticity in peripheral reorganization has been ascribed to the changing demands of the environment, specifically in response to appropriate stimulation during critical developmental periods (Hubel and Wiesel, 1970; Cummings and Brunjes, 1997; Hill and May, 2007; Yan, 2003; Ruthazer and Aizenman 2010). Similar activity-dependent mechanisms could be involved when lateral line afferent neurons selectively establish contacts with hair cells of only one polarity. While initial target selection of afferent neurons onto hair cells is stochastic (Faucherre et al., 2009; Nagiel et al., 2009), it has been suggested that hair cell activity subsequently decreases the establishment of afferent synapses onto hair cells such that further contacts are exclusively established onto hair cells with the same polarity (Faucherre et al., 2010).

Organization in the hindbrain

Since a robust somatotopy exists in the larval lateral line system (Alexandre and Ghysen, 1999; Gompel et al., 2001), we investigated how this organization in turn relates to a known postsynaptic target in the hindbrain—the Mauthner cell. We found that afferent central projections from widely separated neuromasts do not occupy segregated regions when they converge onto the lateral dendrite of the Mauthner cell. Thus, the gross somatotopy of the system is less obvious close to the Mauthner cell. Our interpretation is that spatially organized input from the lateral line to the Mauthner cell is less critical at early stages of development, when the ability to escape quickly is more important than the fine control of the escape direction (Nissanov et al., 1990). In addition, there were no obvious contacts onto Mauthner cell homologs, which are serial reticulospinal cells that play a role in controlling the directionality of the escape response (Foreman and Eaton, 1993; O'Malley et al., 1996). We anticipate that lateral line input to these Mauthner cell homologs may serve to fine tune the directionality of the escape later in development.

ACKNOWLEDGMENTS

We thank Joseph Fetcho at Cornell University, Hitoshi Okamoto of the RIKEN Brain Science Institute, and the National Bioresource Project of Japan for providing zebrafish strains. We thank members of the Whitney Laboratory for Marine Bioscience for their comments on an earlier version of the article. We thank Katherine DeCesare and Christina Walker for excellent care in maintaining and breeding fish.

LITERATURE CITED

Alexandre D, Ghysen A. 1999. Somatotopy of the lateral line projection in larval zebrafish. Proc Natl Acad Sci U S A 96: 7558–7562.

Chiba A, Shepherd D, Murphey RK. 1988. Synaptic rearrangement during postembryonic development in the cricket. Science 240:901–905.

Corey DP, Hudspeth AJ. 1979. Ionic basis of the receptor potential in a vertebrate hair cell. Nature 281:675–677.

Cummings DM, Brunjes PC. 1997. The effects of variable periods of functional deprivation on olfactory bulb development in rats. Exp Neurol 148:360–366.

Faber DS, Korn H. 1975. Inputs from the posterior lateral line nerves upon the goldfish Mauthner cells. II. Evidence that the inhibitory components are mediated by interneurons of the recurrent collateral network. Brain Res 96:349–356.

Faucherre A, Baudoin J-P, Pujol-Martí J, López-Schier H. 2010. Multispectral four-dimensional imaging reveals that evoked activity modulates peripheral arborization and the selection of plane-polarized targets by sensory neurons. Development 137:1635–1643.

Faucherre A, Pujol-Martí J, Kawakami K, López-Schier H. 2009. Afferent neurons of the zebrafish lateral line are strict selectors of hair-cell orientation. PloS One 4:e4477.

Flock A, Wersall J. 1962. A study of the orientation of the sensory hairs of the receptor cells in the lateral line organ of fish, with special reference to the function of the receptors. J Cell Biol 15:19–27.

Foreman MB, Eaton RC. 1993. The direction change concept for reticulospinal control of goldfish escape. J Neurosci 13: 4101–4113.

Ghysen A, Dambly-Chaudière C. 2004. Development of the zebrafish lateral line. Curr Opin Neurobiol 14:67–73.

Ghysen A, Dambly-Chaudière C. 2007. The lateral line microcosmos. Genes Dev 21:2118–2130.

Gompel N, Cubedo N, Thisse C, Thisse B, Dambly-Chaudière C, Ghysen A. 2001. Pattern formation in the lateral line of zebrafish. MOD 105:69–77.

Harrison RG. 1904. Experimentelle Untersuchung ueber die Entwicklung der Sinnesorgane der Seitenlinie bei den Amphibien. Arch Mikrosk Anat 63:35–149.

Hill DL, May OL. 2007. Development and plasticity of the gustatory portion of nucleus of the solitary tract. In: Bradley RM, editors. The role of the nucleus of the solitary tract in gustatory processing. Boca Raton, FL: CRC Press.

Howard J, Hudspeth AJ. 1987. Mechanical relaxation of the hair bundle mediates adaptation in mechanoelectrical transduction by the bullfrog's saccular hair cell. Proc Natl Acad Sci U S A 84:3064–3068.

Hubel DH, Wiesel TN. 1970. The period of susceptibility to the physiological effects of unilateral eye closure in kittens. J Physiol 206:419–436.

Korn H, Faber DS. 1975. Inputs from the posterior lateral line nerves upon the goldfish Mauthner cell. I. Properties and synaptic localization of the excitatory component. Brain Res 96:342–348.

Korn H, Faber DS, Mariani J. 1974. Existence of projections of posterior nerves from the lateral line on the Mauthner cell; their antagonistic effect on the activation of this neuron by vestibular afferences. C R Acad Sci Hebd Seances Acad Sci D 279:413–416.

Ledent V. 2002. Postembryonic development of the posterior lateral line in zebrafish. Development 129:597–604.

LeMasurier M, Gillespie PG. 2005. Hair-cell mechanotransduction and cochlear amplification. Neuron 48:403–415.

Liao JC. 2010. Organization and physiology of posterior lateral line afferent neurons in larval zebrafish. Biol Lett 6:402–405.

Metcalfe WK, Kimmel CB, Schabtach E. 1985. Anatomy of the posterior lateral line system in young larvae of the zebrafish. J Comp Neurol 233:377–389.

Mohr C, Görner P. 1996. Innervation patterns of the lateral line stitches of the clawed frog, Xenopus laevis, and their reorganization during metamorphosis. Brain Behav Evol 48:55–69.

Nagiel A, Andor-Ardó D, Hudspeth AJ. 2008. Specificity of afferent synapses onto plane-polarized hair cells in the posterior lateral line of the zebrafish. J Neurosci 28:8442–8453.

Nagiel A, Patel SH, Andor-Ardó D, Hudspeth AJ. 2009. Activity-independent specification of synaptic targets in the posterior lateral line of the larval zebrafish. Proc Natl Acad Sci U S A 106:21948–21953.

Nissanov J, Eaton RC, DiDomenico R. 1990. The motor output of the Mauthner cell, a reticulospinal command neuron. Brain Res 517:88–98.

Nuñez VA, Sarrazin AF, Cubedo N, Allende ML, Dambly-Chaudière C, Ghysen A. 2009. Postembryonic development of the posterior lateral line in the zebrafish. Evol Dev 11: 391–404.

O'Malley DM, Kao YH, Fetcho JR. 1996. Imaging the functional organization of zebrafish hindbrain segments during escape behaviors. Neuron 17:1145–1155.

Raible DW, Kruse GJ. 2000. Organization of the lateral line system in embryonic zebrafish. J Comp Neurol 421: 189–198.

Ruthazer ES, Aizenman CD. 2010. Learning to see: patterned visual activity and the development of visual function. Trends Neurosci 33:183–192.

Sapède D, Gompel N, Dambly-Chaudière C, Ghysen A. 2002. Cell migration in the postembryonic development of the fish lateral line. Development 129:605–615.

Sarrazin AF, Nuñez VA, Sapède D, Tassin V, Dambly-Chaudière C, Ghysen A. 2010. Origin and early development of the posterior lateral line system of zebrafish. J Neurosci 30:8234–8244.

Sato T, Takahoko M, Okamoto H. 2006. HuC:Kaede, a useful tool to label neural morphologies in networks in vivo. Genesis 44:136–142.

Sato A, Koshida S, Takeda H. 2010. Single-cell analysis of somatotopic map formation in the zebrafish lateral line system. Dev Dyn 239:2058–2065.

Schilling TF. 2002. The morphology of larval and adult zebrafish. In: Nuesslein-Volhard C, Dahm R, editors. Zebrafish, practical approach. Oxford, New York: Oxford University Press. p 59–94.

Webb JF, Shirey JE. 2003. Postembryonic development of the cranial lateral line canals and neuromasts in zebrafish. Dev Dyn 228:370–385.

Wright MR. 1951. The lateral line system of sense organs. Q Rev Biol 26:264–280.

Yan J. 2003. Canadian Association of Neuroscience Review: development and plasticity of the auditory cortex. Can J Neurol Sci 30:189–200.